Title
RANDOM CHOICE METHODS WITH APPLICATIONS TO REACTING GAS FLOW

Author
Chorin, Alexandre Joel.

Publication Date
1976-11-01

To be submitted for Publication

LBL-5557
Preprint

RANDOM CHOICE METHODS WITH APPLICATIONS TO REACTING GAS FLOW

Alexandre Joel Chorin

November 1976

Prepared for the U. S. Energy Research and Development Administration under Contract W-7405-ENG-48

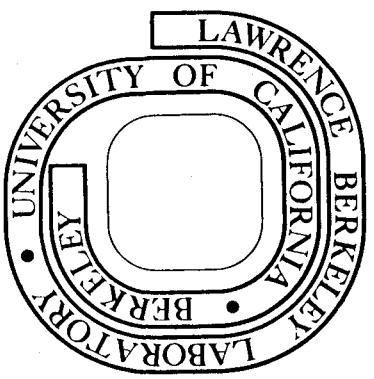

DISCLAIMER

RANDOM CHOICE METHODS WITH APPLICATIONS TO REACTING GAS FLOW

Alexandre Joel Chorin*

Department of Mathematics and Lawrence Berkeley Laboratory
University of California
Berkeley, California 94720

*Partially supported by the Office of Naval Research under Contract No. N00014-76-C-0316, and by the U.S. ERDA.

Abstract

The random choice method is analyzed; appropriate boundary conditions are described, and applications to reacting gas flow in one dimension are carried out. These applications illustrate the advantages of the method.

Introduction

The random choice method for solving hyperbolic systems was introduced as a numerical tool in [2]. It grew from a constructive existence proof due to Glimm [5]. In this method, the solution of the equations is constructed as a superposition of locally exact elementary similarity solutions; the superposition is carried out through a sampling procedure. The computing effort per mesh point is relatively large, but the global efficiency is high when the solutions sought contain components of widely differing time scales. This efficiency is due to the fact that the appropriate interactions can be properly taken into account when the elementary similarity solutions are computed. The aim of the present paper is to provide a further analysis of the method, and to illustrate its usefulness in the analysis of reacting gas flow. Examples are given of detonation and deflagration waves, with infinite and finite reaction rates.

We begin by describing the method briefly. Consider the hyperbolic system of equations

$$\underline{v}_t = (\underline{f}(\underline{v}))_x \ , \ \underline{v}(x,0) \ \text{ given} \ , \tag{1}$$

when $\underline{v}$ is the solution vector, and subscripts denote differentiation. The time t is divided into intervals of length k. Let h be a spatial increment. The solution is to be evaluated at the points (ih,nk) and $((i+\frac{1}{2})h,(n+\frac{1}{2})k)$, $i = 0,\pm1,\pm2,\ldots$, $n = 1,2,\ldots$. Let $\underline{u}_i^n$ approximate $\underline{v}(ih,nk)$, and $\underline{u}_{i+1/2}^{n+1/2}$

approximate $\underline{v}((i+\frac{1}{2})h,(n+\frac{1}{2})k)$. The algorithm is defined if $\underline{u}_{i+1/2}^{n+1/2}$ can be found when $\underline{u}_i^n$, $\underline{u}_{i+1}^n$ are known. Consider the following Riemann problem:

$$\underline{v}_t = (f(\underline{v}))_x \ , \ t > 0 \ , \ -\infty < x < +\infty \ ,$$

$$\underline{v}(x,0) = \begin{cases} \underline{u}_{i+1}^n & \text{for } x \geq 0 \ , \\ \underline{u}_i^n & \text{for } x < 0 \ . \end{cases}$$

Let $\underline{w}(x,t)$ denote the solution of this problem. Let θ_i be a value of a variable θ , $-\frac{1}{2} \leq \theta \leq \frac{1}{2}$. Let P_i be the point $(\theta_i h,\frac{k}{2})$, and let

$$\tilde{\underline{w}} = \underline{w}(P_i) = \underline{w}(\theta_i h,\frac{k}{2})$$

be the value of the solution $\underline{w}$ of the Riemann problem at P_i . We set

$$\underline{u}_{i+1/2}^{n+1/2} = \tilde{\underline{w}} \ .$$

In other words, at each time step, the solution is first approximated by a piecewise constant function; it is then advanced in time exactly, and new values on the mesh are obtained by sampling. The usefulness of the method depends on the possibility of solving Riemann problems efficiently.

Simple examples and partial error estimates

In order to explain the method further and analyze its limitations, we consider in this section simple examples of its use; the first one was already discussed in [7]. Consider the equation

$$v_t = v_x \tag{2}$$

in $-\infty < x < +\infty$, $t > 0$, with $v(x,0) = g(x)$ given. One can readily see that if a single θ is picked per half time step, Glimm's method reduces to

$$u_{i+1/2}^{n+1/2} = \begin{cases} u_{i+1}^{n} & \text{if} \quad \theta h \geq -k/2 \\ u_{i}^{n} & \text{if} \quad \theta h < -k/2 \end{cases} .$$

It follows that

$$u_i^n = v(ih+\eta,t) ,$$

where $\eta = \eta(t)$ is a random variable which depends on t alone; i.e., the computed solution equals the exact solution with a shift independent of x . The magnitude of η depends on the choices of θ . Consider the following strategies for picking θ :

i) θ is picked at random from the uniform distribution on $[-\frac{1}{2},\frac{1}{2}]$;

ii) n is assumed known in advance; the interval $[-\frac{1}{2},\frac{1}{2}]$ is divided into n subintervals of equal lengths and θ_i is picked in the middle of the i^{th} subinterval;

iii) (A compromise between i) and ii)): $[-\frac{1}{2},\frac{1}{2}]$ is divided into m subintervals, $m << n$, and θ_1 is picked at random in the first subinterval, θ_2 in the second subinterval, θ_{m+1} in the first subinterval, etc.

A fourth strategy which relies on the well-equipartitioned sequences studied by Richtmyer and Ostrowski was suggested by Lax [6], but is not useful in the present context.

If strategy i) is used, we have

$$x+\eta = \text{displacement of the initial value}$$

$$= \sum_{i=1}^{2n} \eta_i \ ,$$

where

$$\eta_i = \begin{cases} \frac{h}{2} & \text{if } h\theta_i < -k/2 \\ -\frac{h}{2} & \text{if } h\theta_i \geq -k/2 \ . \end{cases}$$

The variance of η_i is readily evaluated:

$$\text{var}(\eta_i) = \frac{h^2}{4}\,(1-\frac{k}{h})(1+\frac{k}{h}) \quad ;$$

the variance of η is thus

$$\frac{nh^2}{4}(1-\frac{k}{h})(1+\frac{k}{h}) ,$$

and the standard deviation of η, which measures its magnitude, is $\frac{\sqrt{n}h}{2}\{(1-\frac{k}{h})(1+\frac{k}{h})\}^{1/2} = 0(\sqrt{n}h)$.

If the second strategy is used,

$$u_i^n = v(x+\eta,t) , \quad |\eta| \leq \frac{1}{2n} ,$$

if $n = 0(h^{-1})$, $\eta = 0(h)$. If the third strategy is used, and n is a multiple of m, $\eta = 0(h\sqrt{n/m})$, since only in every m^{th} half step is the outcome of the sampling in doubt.

Assume v is of compact support. Following a suggestion by Lax, we define the resolution of the scheme by

$$Q^{-1} = \min_q \|u_i^n - v(ih+q,t)\|$$

where $\| \|$ denotes the maximum norm. The scheme has resolution of order m if $Q = 0(h^{-m})$. The displacement d of the scheme is defined by

$$Q^{-1} = \|u_i^n - v(ih+d,t)\|$$

$$= \min_q \|u_i^n - v(ih+q,t)\| .$$

The method applied to the present problem has almost first order accuracy, almost first order displacement, but infinite resolution. There is no smoothing and no numerical diffusion or dispersion. For any k/h, the domain of dependence of a point is always a single point. The answers are always bounded. If the Courant condition $k/h \leq 1$ is violated, the equation being approximated is $v_t = (h/k)v_x$. Clearly, since these results are independent of k/h, they generalize to hyperbolic systems with constant coefficients.

Consider now the equation

$$v_t = a(x,t)v_x ,$$

in $-\infty < x < +\infty$, $t > 0$, $v(x,0) = g(x)$ given, and $a(x,t)$ a Lipschitz continuous function of both x and t. The method is not well suited to the solution of such an equation, both because the solution of the Riemann problem requires a possibly laborious integration of a characteristic equation, and because the rrors will turn out to be large compared with those incurred in other available methods. The analysis is nevertheless illuminating.

Let C_{x_0} be the characteristic

$$\frac{dx}{dt} = -a(x,t) , \quad x(0) = x_0 .$$

For each i, we have

$$u_{i+1/2}^{n+1/2} = \begin{cases} u_i^n & \text{if } P = (\theta h, \frac{k}{2}) \text{ lies to the right of } C_{(1+\frac{1}{2})h} \\ u_{i+1}^n & \text{if } P \text{ lies to the left of } C_{(i+\frac{1}{2})h} \end{cases} .$$

As before,

$$u_i^n = v(x+\eta,t) \ , \ x = ih \ , \ t = nk \ ;$$

where η is a random variable which now depends on both x and t .

If θ is picked at random from the uniform distribution on $[-\frac{1}{2},\frac{1}{2}]$ (Strategy i)) we have as before $\eta = 0(h\sqrt{n})$. Strategy ii) clearly yields an error $0(1)$. Strategy iii) is more advantageous; the standard deviation of η is again bounded by $0(h\sqrt{n/m})$. However, the mean of η is no longer zero. Assume $k = 0(h)$. Note that $a(x,t)$ may vary by $0(mh)$ before this change affects the values of η . Thus, $\bar{\eta}$ = mean of $\eta = 0(mh)$, and $\eta = 0(mh) + 0(h\sqrt{n/m})$. If $n = 0(h^{-1})$ and $m = 0(n^{1/3})$, then $\eta = 0(h^{2/3})$. We have less than first order accuracy and more than first order displacement.

We now try to assess the relative displacement of two points. Let us assume that the first sampling strategy is used, i.e., θ is picked at each step from the uniform distribution on $[-\frac{1}{2},\frac{1}{2}]$. Consider first the quantity

$$\Delta\eta(h,k) = (\eta(x,t+k) - \eta(x+th,t+k))$$

$$- (\eta(x,t)-\eta(x+h,t)) \ ,$$

i.e., the difference between the numerically induced translations experienced by two neighboring points during one time step. If $\Delta\eta(h,k) > 0$, information is lost: one value of $v(x,0)$ disappears. If $\Delta\eta(h,k) < 0$, a false constant state is created. $\Delta\eta(h,k)$ can take on the values $0,\pm h$. $\Delta\eta(h,k) \neq 0$ if $P = (\theta h, \frac{k}{2})$ falls to the left of the characteristic through one of the points $(ih,nk),((i+1)h,nk)$ and to the right of the other. This happens with probability $0(h)$. I.e., the variance of $\Delta\eta(h,k)$ is $0(h^3)$. Therefore, the variance of $\Delta\eta(h) = \eta(x,t) - \eta(x+h,t)$ is $n0(h^3) = 0(h^2)$ if $n = 0(h^{-1})$, and the standard deviation of $\Delta\eta(h)$ is $0(h)$, i.e., neighboring values in the range of v do not fly far apart. The same estimate holds for the other sampling strategies.

Consider now the relative displacement $\Delta\eta$ of two values far apart. Let $\eta_1 = \eta(x,t)$, $\eta_2 = \eta(x+X,t)$, and $\Delta\eta = \eta_2 - \eta_1$, and thus

$$u_i^n = v(x+\eta_1,t) = g(x_1) \ , \ ih = x \ , \ nk = t \ ,$$

$$u_{i+i_0}^n = v(x+X+\eta_2,t) = g(x_2) \ , \ i_0 h = X \ ,$$

where $g(x) = v(x,0)$. Let C_{x_1} be the characteristic through

$(x_1,0)$, and similarly for C_{x_2} . x_2-x_1 has increased by $\pm$ h each time $P = (\theta h,\frac{k}{2})$ fell between the two characteristics. Assume the first sampling strategy is used. There are two sources of error which make $\Delta\eta \neq 0$. There is the standard deviation of the sum of the random variables which equal $\pm$ h when P is between the characteristics, and are zero otherwise, (this is clearly $0(h\sqrt{n})$) , and there is the uncertainty in the slope of the characteristics due to the lateral displacement of the solution; this is again $0(h\sqrt{n})$ and induces an error $0(h^{3/2}n^{3/4}) = 0((h\sqrt{n})^{3/2})$; if $n = 0(h^{-1})$, this is $0(h^{3/4})$. Thus $\Delta\eta = 0(h\sqrt{n})$, and the resolution is not of higher order than the accuracy. Similar results hold for the other sampling strategies.

We now turn to the nonlinear problem

$$\underline{v}_t = (f(\underline{v}))_x ,$$

where f is a function of v but not explicitly a function of x and t . The method of analysis we have used here is not applicable, since values of $\underline{v}$ are not merely propagated along characteristics. Furthermore, we have here no way of taking into account properly the fact that rarefaction or loss of information incurred in the numerical process correspond to genuine properties of the differential equations. All we can provide here is a heuristic analysis. Consider the third sampling strategy. Since the slope of the characteristic depends on the values of v and not on x , and values of v at neighboring points

remain attached to neighboring points, we expect the term $O(mh)$ in η to disappear, and have $\eta = O(h\sqrt{n/m})$. Thus, the resolution should be at least $O(h\sqrt{n/m})$. Note that if $n = O(h^{-1})$ and $m = O(n)$, the random element in the method loses its significance.

In the case of a shock separating two constant states, one can readily see that $d = O(h\sqrt{n/m})$ but the resolution is infinite. One can trivially define resolution in a neighborhood. Thus, what we have is a rather awkward first order method, which resolves shocks very sharply. We also know that it keeps fluid interfaces perfectly sharp [2]. It is useful for the analysis of problems in cartesian coordinates in which the dynamics of the discontinuities are of paramount significance. We shall provide examples of such problems in later sections. Recent results (see, e.g., [8]) show that in such problems substantially higher accuracy cannot be achieved.

Boundary conditions

The correct imposition of boundary conditions in our method requires careful thought, and was not adequately discussed in [2]. It is clear that even in the case of equation (2) the presence of a boundary can detract from both accuracy and resolution. The lateral displacement of the solution may make some function values disappear across the boundary and care must be taken to

ensure the possibility of their retrieval. Additional storage across the boundary and careful accounting of the lateral displacement provide a remedy.

The following procedure has been introduced in [2] to reduce the lateral displacement of the solution (and thus reduce the loss of information at walls), when the third sampling strategy is used. The goal is to obtain as fast as possible solution values on both sides of whatever wave pattern emerges in the solution of the Riemann problem, and thus rapidly offset a displacement to right by a displacement to the left (or vice versa). We pick an integer $m' < m$, m and m' mutually prime, and n_0 integer, $n_0 < m$, and construct the sequence of integers

$$n_{i+1} = (n_i+m')(\text{mod } m) \quad . \tag{3}$$

The subintervals of $[-\frac{1}{2},\frac{1}{2}]$ are them sampled in the order $n_0,n_1,n_2,\ldots$ rather than in the natural succession. One can further modify the sampling so that of two successive values of θ, one lies in $[-\frac{1}{2},0]$ and one in $[0,\frac{1}{2}]$. These procedures do not increase the error far from the wall, and are quite effective, although no analytical assessment of their efficiency is available.

Suppose we are solving the equations of gas dynamics (equations (4) below), and using the third sampling strategy, modified by (3) or not. Assume the velocity v is given at the

boundary. One can find a state (i.e., a set of values for the gas variables) which has the given velocity and which can be connected to the state one mesh point into the fluid by a simple wave (see, e.g., [4]). This is equivalent to solving half a Riemann problem, and provides an appropriate solution field which can be sampled. The same result can be obtained by symmetry considerations. Consider a boundary point to the right on the region of flow; let the boundary conditions be imposed at a point $i_0 h$. A fake right state at $(i_0+\frac{1}{2})h$ is created, with

$$\rho_{i_0+1/2} = \rho_{i_0-1/2} ,$$

$$v_{i_0+1/2} = 2V - v_{i_0-1/2} ,$$

$$p_{i_0+1/2} = p_{i_0-1/2} ,$$

where ρ,v,p are respectively the gas density, velocity and pressure, and V is the velocity of the wall. The constant state in the middle of the Riemann solution is the wall state, and it is sampled to the left of the slip line $\frac{dx}{dt} = V$.

This procedure contains a pitfall, not noticed in [2]; let θ be chosen in accordance with our usual sampling strategy; let θ_1,θ_2 be the values of θ at two successive time steps (θ_1 and θ_2 are not independent). θ_1',θ_2' , the values used at the wall, differ from θ_1 and θ_2 since only

part of the interval $[-\frac{1}{2},\frac{1}{2}]$ is sampled (or else one does not remain to the left of the wall line $\frac{dx}{dt} = V$). θ_1' and θ_2' can presumably be obtained by a linear change of variables. Consider a specific part of the wave pattern at the wall. Since θ_1',θ_2' are not independent, the possibility exists that whenever θ_1' picks up the specific part we are considering, θ_2' is such that this information is lost to the wall. This possibility was not noticed in [2], and its removal by the methods whose description follows contributes to the sharpening of the results obtained in [2].

It is always consistent to pick θ_1',θ_2' by a linear change of variables from two values picked independently from the uniform distribution on $[-\frac{1}{2},\frac{1}{2}]$. On the average no information will be lost to the wall, but the variance of the solution will be increased. Better strategies can be devised, but require thought in each special case. If the walls are at rest, $V = 0$, one can proceed as follows: impose the boundary condition on the right at time nk and a point i_1h, and on the left at time $(n+\frac{1}{2})k$ at a point $(i_2+\frac{1}{2})h$, i_1,i_2 integers. One can see that if θ_1,θ_2 are so chosen that $\theta_1 \leq 0$ at time nk, and $\theta_2 \geq 0$ at time $(n+\frac{1}{2})k$, then θ_1 and θ_2 can be used at the boundary as well as in interior without loss of resolution.

Detonations and deflagrations in a one dimensional ideal gas

Our goal in this section is to present a quick summary of

the elementary theory of one dimensional detonation and deflagration waves, (for more detail, see, e.g., [4] and [10]), and then derive some relations between the hydrodynamical variables on the two sides of such waves for later use.

The equations of gas dynamics are

$$\rho_t + (\rho v)_x = 0 \quad , \tag{4a}$$

$$(\rho v)_t + (\rho v^2 + p)_x = 0 \quad , \tag{4b}$$

$$e_t + ((e+p)v)_x = 0 \quad , \tag{4c}$$

where the subscripts denote differentiation, ρ is the density of the gas, v is the velocity, ρv is the momentum, e is the energy per unit volume and p is the pressure. We have

$$e = \rho\varepsilon + \frac{1}{2}\rho v^2 \quad , \tag{4d}$$

where $\varepsilon = \varepsilon_i + q$, ε_i is the internal energy per unit mass,

$$\varepsilon_i = \frac{1}{\gamma-1}\frac{p}{\rho} \tag{4e}$$

where γ is a constant, $\gamma > 1$, and q is the energy of formation which can be released through chemical reaction (see [4]). In the present section it will be assumed that part of q is released instantaneously in an infinitely thin reaction zone. Let the subscript 0 refer to unburned gas (i.e., gas which has

not yet undergone the chemical reaction) and let the subscript 1 refer to burned gas. The unburned gas is on the right. We have

$$\varepsilon_1 = \frac{1}{\gamma_1 - 1}\frac{p_1}{\rho_1} + q_1$$

$$\varepsilon_0 = \frac{1}{\gamma_0 - 1}\frac{p_0}{\rho_0} + q_0 \quad .$$

For the sake of simplicity, we shall make here the unrealistic assumption $\gamma_1 = \gamma_0 = \gamma$. (The case $\gamma_1 \neq \gamma_0$ is more difficult only because of additional algebra.) When $\gamma_1 = \gamma_0 = \gamma$ the reaction can be exothermic (i.e., release energy) only if $q_1 > q_0$.

Let U be the velocity of the reaction zone. Let

$$w_1 = v_1 - U$$

$$w_0 = v_0 - U \quad .$$

Conservation of mass and momentum is expressed by

$$\rho_1 w_1 = \rho_0 w_0 = -M \tag{5}$$

$$\rho_0 w_0^2 + p_0 = \rho_1 w_1^2 + p_1 \tag{6}$$

(see [4]). From these relations one readily deduces

$$M^2 = -\frac{p_0 - p_1}{\tau_0 - \tau_1} \text{ , where } \tau = 1/\rho \ .$$

Define the function H by

$$H = \varepsilon_1 - \varepsilon_0 + \frac{(\tau_0 - \tau_1)}{2}(p_1 + p_0) \quad .$$

Conservation of energy is expressed by

$$H = H(\tau_1, p_1, \tau_0, p_0) = 0 \quad .$$

Define $\Delta = q_0 - q_1$, ($\Delta \leq 0$ for an exothermic process), and $\mu^2 = \frac{\gamma - 1}{\gamma + 1}$; we find

$$\begin{aligned} 2\mu^2 H = 0 &= (1-\mu^2)\tau_0 p_0 - (1-\mu^2)p_1\tau_1 - 2\mu^2\Delta \\ &\quad + \frac{(\tau_0 - \tau_1)}{2}(p_1 + p_0) \qquad (7) \\ &= p_0(\tau_0 - \mu^2\tau_1) - p_1(\tau_1 - \mu^2\tau_0) - 2\mu^2\Delta \quad . \end{aligned}$$

In the (τ_1, p_1) plane the locus of points which can be connected to (τ_0, p_0) by an infinitely thin combustion wave is a curve which reduces to a hyperbola when Δ is independent of p and τ . (See Figure 1.) The lines through (τ_0, p_0) tangent to $H = 0$ are called the Rayleigh lines. Their points of tangency, S_1 and S_2 , are called the Chapman-Jouguet (CJ) points. A portion of the curve is omitted because it corresponds to unphysical events in which $M^2 < 0$. The upper portion of the curve corresponds to detonations; the portion above S_1 to strong

detonations and the portion below to weak detonations. The lower part of the curve corresponds to deflagrations.

The velocity and strength of a strong detonation are entirely determined by the state of the unburned gas in front of the detonation and one quantity behind the detonation, just as in the case with shocks. Let p_0 , ρ_0 , τ_0 , ε_0 and v_0 be given, as well as p_1 , and assume the unburned gas lies to the right of the detonation. We have from (7)

$$\tau_1 = \tau_0\left(\frac{p_0+\mu^2 p_1}{\mu^2 p_0+p_1}\right) + \frac{2\mu^2\Delta}{\mu^2 p_0+p_1} \tag{8}$$

and thus

$$M^2 = \frac{p_0-p_1}{\tau_0-\tau_1} = \frac{p_0-p_1}{\tau_0\left(\frac{p_0+\mu^2 p_1}{p_1+\mu^2 p_0} + \frac{2\mu^2\Delta}{\mu^2 p_0+p_1} - 1\right)} \quad ;$$

Let $[p] = p_1-p_0$; some algebra yields

$$M^2 = p_0\rho_0\left(\frac{\gamma-1}{2} + \frac{\gamma+1}{2}\left(\frac{p_1}{p_0}\right)\right)/\left(1-(\gamma-1)\rho_0\Delta/[p]\right) \quad . \tag{9}$$

If $\Delta = 0$ this formula reduces to the expression for M in a shock, as given in [2] or [9]. M is real if $[p]-(\gamma-1)\rho_0\Delta \geq 0$; this can be readily seen to hold in a strong detonation.

The states on the curve $H = 0$ located between the CJ point S_1 and the line $\tau = \tau_0$ correspond to weak detonations. As described in [4], the state behind a weak detonation is

entirely determined by the velocity U of the detonation and the state in front of it. In fact, a weak detonation cannot occur and what does happen is a CJ detonation followed by a rarefaction wave. Our next objective is to derive an explicit criterion for determining whether a detonation will be a strong detonation or a CJ detonation.

It is shown in [4] that at S_1, $|w_1| = c_1$ where $c_1 = \sqrt{\gamma p_1/\rho_1}$ is the sound speed, i.e., a CJ detonation moves with respect to the burned gas with a velocity equal to the velocity of sound in the burned gas. We now use this fact to determine the density ρ_{CJ}, velocity v_{CJ} and pressure p_{CJ} behind a CJ detonation.

From equations (4) and (5) one finds

$$\frac{p_1-p_0}{\tau_1-\tau_0} = -\rho_1^2 w_1^2 = -\rho_0^2 w_0^2 = -M^2 \quad ,$$

and thus in a CJ detonation

$$\frac{p_1-p_0}{\tau_1-\tau_0} = -\rho_1^2 \frac{\gamma p_1}{\rho_1} = -\gamma p_1/\tau_1 \, , \quad \tau_1 = 1/\rho_1 \quad ,$$

or

$$\tau_1(p_1(1+\gamma)-p_0) = \gamma \tau_0 p_1 \, . \tag{10}$$

Equating τ_1 obtained from (8) to τ_1 in (10), we find

$$\tau_0\left(\frac{\mu^2 p_1+p_0}{p_1+\mu^2 p_0}\right)+\frac{2\mu^2\Delta}{(p_1+\mu^2 p_0)}=\frac{\gamma\tau_0 p_1}{p_1(1+\gamma)-p_0} \quad .$$

Some algebra reduces this equation to

$$p_1^2 + 2p_1 b + c = 0 \quad ,$$

where

$$b = -p_0 - 2\Delta(\gamma-1)\rho_0 \tag{11a}$$

$$c = p_0^2 + 2\mu^2 p_0\rho_0\Delta \quad ; \tag{11b}$$

a trivial calculation shows that $b^2-c \geq 0$ if $\gamma \geq 1$ and $\Delta \leq 0$. Thus

$$p_{CJ} = p_1 = -b + \sqrt{b^2-c} \tag{11c}$$

where the + sign is mandatory since a detonation is compressive. Given $p_{CJ} = p_1$, $\rho_{CJ} = \rho_1 = \tau_1^{-1}$ can be obtained from equation (10). Since $M = -\rho_1 w_1$, and $w_1 = -c_1$, we find

$$M = \sqrt{\gamma p_1 \rho_1} = \sqrt{\gamma p_{CJ}\rho_{CJ}} \quad .$$

The velocity U_{CJ} of the detonation is found from

$$\rho_0(v_0-U_{CJ}) = -M$$

which yields $U_{CJ} = (\rho_0 v_0 + \sqrt{\gamma p_{CJ} \rho_{CJ}})/\rho_{CJ}$, and then

$$v_{CJ} = U_{CJ} - c_{CJ} \quad . \tag{12}$$

v_{CJ} depends only on the state of the unburned gas.

Suppose v_1 , the velocity of the burned gas, is given. If $v_1 \leq v_{CJ}$ a CJ detonation will appear, followed by a rarefaction wave. If $v_1 = v_{CJ}$ a CJ detonation will appear alone, and if $v_1 > v_{CJ}$ a strong detonation will take place.

If the unburned gas lies to the left of the burned gas analogous relations are found; the only difference lies in the signs of v , in particular,

$$M = +\rho_1(v_1 - U) = +\rho_0(v_0 - U) \quad .$$

The velocity of a possible deflagration cannot be determined within the context of a theory which assumes the gas to be nonconducting; this point will be further discussed below. It will turn out that for a nonconducting gas the only possible deflagration is a constant pressure deflagration, $p_1 = p_0$, which moves with zero velocity with respect to the gas; i.e., it is indistinguishable from a slip line.

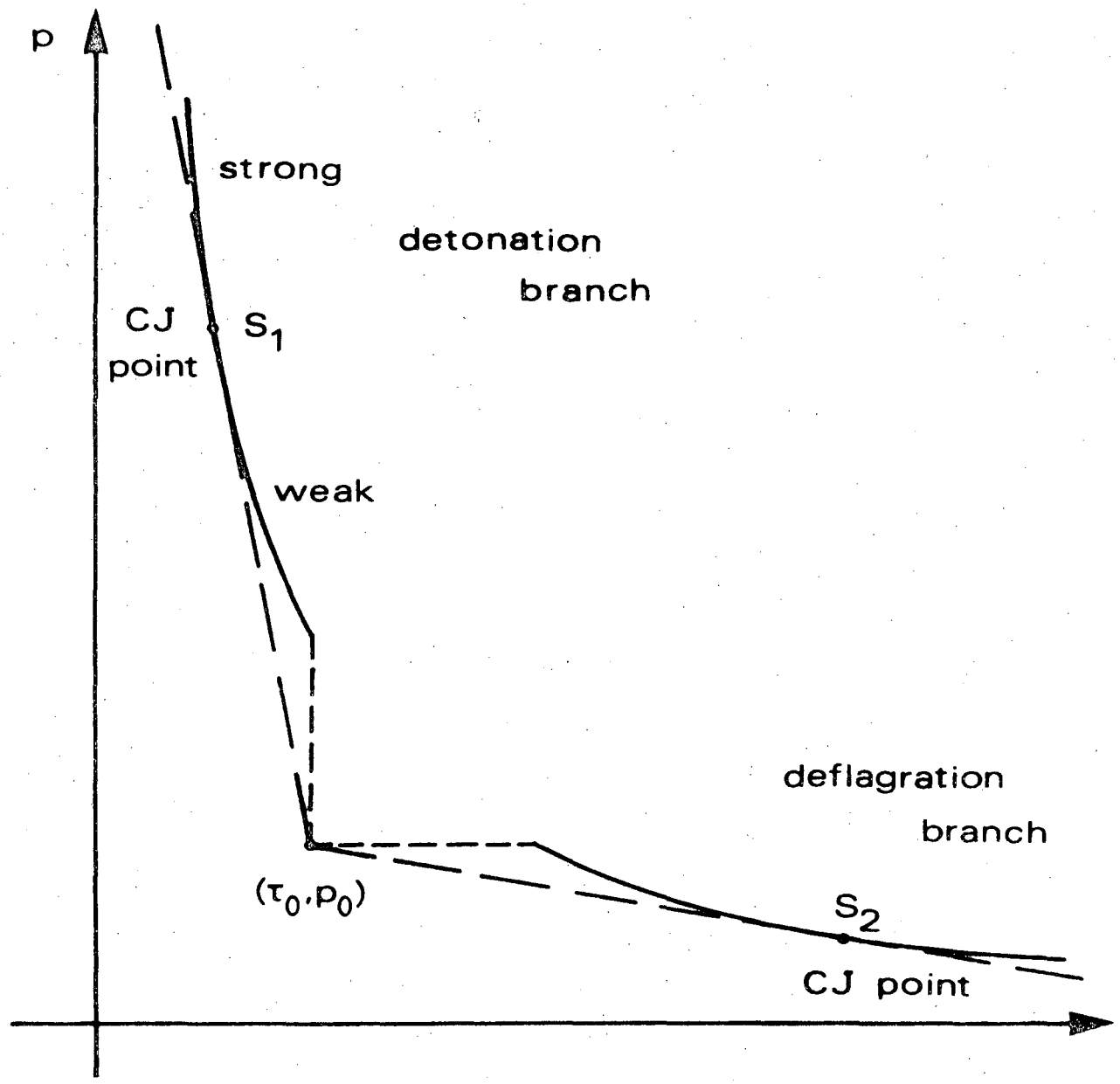
p
strong
detonation
branch
CJ
point
S_1
weak
deflagration
branch
(τ_0, p_0)
S_2
CJ point

Application of the method to reacting gas flow.

One interesting feature of our method is its applicability to the analysis of gas flow in which exothermic chemical reactions are taking place and producing substantial dynamical effects. A Riemann problem is solved at each time step and at each point in time; this solution is then sampled. The advantage of this procedure is that the interaction of the flow and the chemical reaction can be taken into account when the Riemann problem is solved, even when the time scales of the chemistry and the fluid flow are very different. As a result, the basic conservation laws are satisfied at the end of each time step. It can be readily seen that if the chemical reactions and the gas flow were to be taken into account in separate fractional steps, the basic conservation laws may be violated at the end of each hydrodynamical step, thus either inducing unwanted oscillations and waves, or requiring time steps small enough for all changes to be very gradual--usually a costly remedy. It is interesting to note that the Riemann solutions with energy deposition in the flow field are equivalent to the exothermic centers introduced by Oppenheim [3] and serve the same purpose of accounting for the dynamical effects of the exothermic reactions. These discrete exothermic centers correspond to a physical reality whose origin can be ascribed to the fluctuations in the levels of chemical species [1].

We consider here the simplest possible description of a reacting gas (see e.g. [9]):

$$\rho_t + (\rho v)_x = 0 \tag{13a}$$

$$(\rho v)_t + (\rho v^2 + p)_x = 0 \tag{13b}$$

$$e_t + ((e + p)v)_x - \lambda T_{xx} = 0 \tag{13c}$$

where, as before, ρ is the density, v is the velocity, e the energy per unit volume,

$$e = \rho\varepsilon + \frac{1}{2}\rho v^2, \tag{13d}$$

ε is the internal energy. In this section,

$$\varepsilon = \frac{1}{\gamma-1}\frac{p}{\rho} + Zq \tag{13e}$$

where γ is a constant, $\gamma > 1$, q is the total available bonding energy ($q \leqslant 0$), and Z is a progress parameter for the reaction. $T = p/\rho$ is the temperature, and λ is the coefficient of heat conduction. Z is assumed to satisfy the rate equation

$$\frac{dZ}{dt} = -KZ \tag{13f}$$

where

$$\begin{aligned} K &= 0 \quad \text{if} \quad T = p/\rho \leqslant T_0 \ , \\ K &= K_0 \quad \text{if} \quad T = p/\rho > T_0 \ . \end{aligned} \tag{13g}$$

T_0 is the ignition temperature and K_0 is the reaction rate. The equations of the preceding section are recovered if we set $\lambda = 0$, $q = \Delta$, and $K = \infty$.

Equation (13f) is a reasonable prototype of the vastly more complex equations which describe real chemical kinetics. Viscous effects have been omitted here; their inclusion in the present context has little effect and presents little difficulty. (Thus, we assume here a zero Prandtl number.)

The approximation of the dissipation term will be relegated to a separate fractional step, where it is to be handled by straightforward finite differences. In view of (13e), and the perfect gas law $T = p/\rho$ (in appropriate units), this fractional step requires merely the approximation of

$$\partial_t T = (\gamma-1)\, T_{xx}. \tag{14}$$

The differencing of a heat conduction term alone introduces negligible numerical dissipation. Several more sophisticated approximation methods were tried, but did not seem to be worth pursuing.

All that remains to be done is to describe the solution of the Riemann problem for equations (13) with $\lambda = 0$. This will be done with the following simplifying assumption: whatever energy may be released during the time $k/2$ in a portion of the fluid is released instantaneously. This approximation is well in the spirit of our method (since it approximates Z by a piecewise constant function); it also has some physical justification [1].

Solution of a Riemann problem with chemistry.

Our goal is to solve equations (13) and the following data:

$$S_\ell(\rho = \rho_\ell,\ p = p_\ell,\ v = v_\ell,\ Z = Z_\ell) \qquad \text{for } x \leq 0$$

and

$$S_r(\rho = \rho_r,\ p = p_r,\ v = v_r,\ Z = Z_r) \qquad \text{for } x > 0$$

with $\lambda = 0$. We begin by a partial review of the case $K_0 = 0$ (no chemistry; see [2], [6], [9]). The solution consists of a right state S_r, a left state S_ℓ, a middle state $S_*(p = p_*,\ v = v_*)$, separated by waves which are either rarefactions or shocks. S_* is divided by the slip line $\frac{dx}{dt} = v_*$ into two parts with possibly differing values of ρ, ρ_{*_r} to the right of the slip line and ρ_{*_ℓ} to its left. To determine v_* and p_* we proceed as follows: define the quantity

$$M_r = \frac{p_r - p_*}{v_r - v_*} \ . \tag{15}$$

If the right wave is a shock,

$$M_r = -\rho_r(v_r - U_r) = -\rho_{*_r}(v_* - U_r) \tag{16}$$

where U_r is the velocity of the right shock. From the Rankine-Hugoniot conditions one obtains

$$M_r = \sqrt{p_r \rho_r}\,\phi_1(p^*/p_r), \qquad p_*/p_r \geq 1, \tag{17a}$$

where

$$\phi_1(\alpha) = \sqrt{\frac{\gamma+1}{2}\alpha + \frac{\gamma-1}{2}} \tag{17b}$$

If the right wave is a rarefaction, we find

$$M_r = \sqrt{p_r\rho_r}\ \phi_2(p_*/p_r), \quad p_*/p_r \leq 1, \tag{18a}$$

where

$$\phi_2(\alpha) = \frac{\gamma-1}{2\sqrt{\gamma}}\ \frac{1-\alpha}{1-\alpha^{2\gamma/\gamma-1}} \quad . \tag{18b}$$

(18b) is derived through the use of the isentropic law $p\rho^{-\gamma} = \text{constant}$ and the constancy of the right Riemann invariant $\Gamma_r = 2\sqrt{\gamma p/\rho}/(\gamma-1) - v$. The function

$$\phi = \begin{cases} \phi_1(\alpha), & \alpha > 1\ , \\ \phi_2(\alpha), & \alpha < 1\ , \end{cases} \tag{19}$$

is continuous at $\alpha = 1$, with $\phi(1) = \phi_1(1) = \phi_2(1) = \sqrt{\gamma}$. Similarly, we define

$$M_\ell = \frac{p_\ell - p_*}{v_\ell - v_*}\ ; \tag{20}$$

if the left wave is a shock,

$$M_\ell = \rho_\ell(v_\ell - U_\ell) = \rho_{*\ell}(v_* - U_\ell), \tag{21}$$

where U_ℓ is the velocity of the left shock. As on the right, $M_\ell = \sqrt{p_\ell \rho_\ell}\ \phi(p_*/p_\ell)$, where $\phi(\alpha)$ is defined as in equations (17) and (18). From (15) and (20),

$$p_* = (u_\ell - u_r + p_r/M_r + p_\ell/M_\ell)/((1/M_r)+(1/M_\ell)) \tag{22}$$

These considerations lead to the following iteration procedure: Pick a starting value p_*^0 (or values M_r^0, M_ℓ^0), and then compute $p_*^{\nu+1}$, $M_r^{\nu+1}$, $M_\ell^{\nu+1}$, $q \geq 0$ using

$$\tilde{p}^{\nu} = (u_\ell - u_r + p_r/M_r^{\nu} + p_\ell/M_\ell^{\nu})/((1/M_r^{\nu})+(1/M_\ell^{\nu})) \tag{23a}$$

$$p_*^{\nu+1} = \max(\varepsilon, \tilde{p}^{\nu}) \tag{23b}$$

$$M_r^{\nu+1} = \sqrt{p_r \rho_r}\ \phi(p_*^{\nu+1}/p_r) \tag{23c}$$

$$M_\ell^{\nu+1} = \sqrt{p_\ell \rho_\ell}\ \phi(p_*^{\nu+1}/p_\ell) \tag{23d}$$

Equation (23b) is needed because there is no guarantee that in the course of iteration $\tilde{p}$ remains ≥ 0. We usually set $\varepsilon_1 = 10^{-6}$. The iteration is stopped when

$$\max(|M_r^{\nu+1} - M_r^{\nu}|\ ,\ |M_\ell^{\nu+1} - M_\ell^{\nu}|) \leq \varepsilon_2,$$

(we usually picked $\varepsilon_2 = 10^{-6}$); one then sets $M_r = M_r^{\nu+1}$, $M_\ell = M_\ell^{\nu+1}$, and $p_* = p_*^{\nu+1}$.

To start this procedure one needs initial values of either M_r and M_ℓ (or p_*) The starting procedure suggested by Godunov appears to be ineffective, and better results were obtained by setting

$$p_*^0 = (p_r+p_\ell)/2.$$

We also ensured that the iteration was carried out at least twice, to avoid spurious convergence when $p_r = p_\ell$.

As noted by Gudunov, the iteration may fail to converge in the presence of a strong rarefaction. This problem can be overcome by the following variant of Godunov's procedure: If the iteration has not converged after L iterations (we usually set $L = 20$), equation (12b) is replaced by

$$p_*^{\nu+1} = \alpha \max(\varepsilon_1, \tilde{p}^\nu) + (1-\alpha)p_*^\nu \qquad (23b)'$$

with $\alpha = \alpha_1 = \frac{1}{2}$. If a further L iteration occur without convergence, we reset $\alpha_2 = \alpha_1/2$. More generally, the program was written in such a way that if the iteration fails to converge after ℓL iterations (ℓ integer), α is reset to

$$\alpha = \alpha_\ell = \alpha_{\ell-1}/2.$$

In practice, the cases $\ell > 2$ were never encountered. The number of iterations required oscillated between 2 and 10, except at a very few points.

Once p_*, M_r, M_ℓ are known, we have

$$v_* = (p_\ell - p_r + M_r U_r + M_\ell U_\ell)/(M_r + M_\ell) \tag{24}$$

from the definitions of M_r and M_ℓ.

Consider now the case $K_0 \neq 0$, $(\lambda = 0)$; the right and left waves may now be CJ or strong detonations as well as shocks and rarefactions. The task at hand is to incorporate these possibilities into the solution of the Riemann problem.

The state S_r will remain a constant state; v_r and ρ_r are fixed. The energy in S_r must change at constant volume (and thus can do no work). The change δZ_r in Z_r can be found by integrating equations (13f), (13g), with $Z(0) = Z_r$ and $Z(k/2) = Z_r + \delta Z_r$, $\delta Z_r \leq 0$. The new pressure is

$$p_r + \delta p_r = p_r + (\gamma - 1)\delta Z \; q\rho_r \tag{25}$$

(see equation (7). We write $p_r^{new} = p_r + \delta p_r$, and drop the superscript new. (We shall need the old Z_r again and thus refrain from renaming $Z_r + \delta Z_r$.) Similarly, Z_ℓ changes to $Z_\ell + \delta Z_\ell$, and a new p_ℓ is found using the obvious analogue of equation (25).

In S_* the values of Z differ from the values $Z_r + \delta Z_r$, $Z_\ell + \delta Z_\ell$. Let $Z_{*\ell}$ be the value of Z to the left of the slip line and let Z_{*_r} be the value of Z to the right of the slip line. The difference in energy of formation across the right wave is $\Delta_r = (Z_{*_r} - (Z_r + \delta Z_r))q$, and across the left wave it is $\Delta_\ell = (Z_{*\ell} - (Z_\ell + \delta Z_\ell))q$. We shall iterate on the values

$Z_{*\ell}$, Z_{*r}, Δ_r, Δ_ℓ. In the first iteration, we set $Z_{*r} = Z_r + \delta Z_r$, $Z_{*\ell} = Z_\ell + \delta Z_\ell$, and thus $\Delta_r = \Delta_\ell = 0$, and carry out the iterations (23). When (23) has converged, a new pressure p^* is given, and new densities ρ_{*r}, $\rho_{*\ell}$ can be found from equation (16), (21) or the isentropic law. New temperatures $T_{*r} = p_*/\rho_{*r}$, $T_{*\ell} = p_*/\rho_{*\ell}$ are evaluated, equations (13f), (13g) are solved, and new values Z_{*r}, $Z_{*\ell}$, Δ_r, Δ_ℓ are found. If $\Delta_r \leq 0$ the right wave is either a shock or a rarefaction, and if $\Delta_r > 0$ the right wave is either a CJ detonation followed by a rarefaction or a strong detonation.

Let v_* be the velocity in S_*. Given Δ_r, Δ_ℓ, we can find the velocities v_{CJr}, $v_{CJ\ell}$ behind possible CJ detonations on the right and left (equation (12)). If $v_* \leq v_{CJr}$ the right wave is a CJ detonation followed by rarefaction, and if $v_* > v_{CJr}$ the right wave is a strong detonation. The CJ state is unaffected by S_* (since it depends only on S_r) and as far as the Riemann solution is concerned it is a fixed state. If the right wave is a CJ detonation, we redefine M_r,

$$M_r = \frac{p_{CJ}-p_*}{v_{CJ}-v_*},$$

(p_{CJ} from equation (11c)). Then

$$M_r = \sqrt{\rho_{CJ}p_{CJ}}\ \phi_2(p_*/p_{CJ}),\quad p_*/p_{CJ} \leq 1, \tag{26}$$

If the right wave is a strong detonation, we find from (9)

$$M_r = \sqrt{p_r\rho_r}\ \phi_3(\rho_r\Delta_r, p_r, p_*),$$

where

$$(\phi_3(\alpha_1,\alpha_2,\alpha_3))^2 = \frac{\frac{\gamma-1}{2} + \frac{\gamma+1}{2}\frac{\alpha_3}{\alpha_2}}{1 - \frac{(\gamma-1)\,\alpha_1}{\alpha_3-\alpha_2}}$$

Similar expressions occur on the left. The iteration starts with M_r, M_ℓ from the previous iteration, and written out in full, appears as follows:

$$\tilde{p}^{\nu} = (\tilde{v}_\ell - \tilde{v}_r + \tilde{p}_r/M_r^{\nu} + \tilde{p}_\ell/M_\ell^{\nu})/(1/M_r^{\nu} + 1/M_\ell^{\nu}) , \qquad \nu \geq 0,$$

$$p_*^{\nu+1} = \max(\varepsilon,\tilde{p}^{\nu}),$$

$$v_*^{\nu} = (\tilde{p}_\ell - \tilde{p}_r + M_r^{\nu}\tilde{v}_r + M_\ell^{\nu}\,\tilde{v}_\ell)/(M_r^{\nu} + M_\ell^{\nu}),$$

where

$$(\tilde{\rho}_r,\tilde{p}_r,\tilde{v}_r) = \begin{cases} (\rho_{CJr},\ p_{CJr},\ v_{CJr}) & \text{if right wave = CJ detonation,} \\ (\rho_r,\ p_r,\ v_\ell) & \text{otherwise ,} \end{cases}$$

$$(\tilde{\rho}_\ell,\tilde{p}_\ell,\tilde{v}_\ell) = \begin{cases} (\rho_{CJ\ell},\ p_{CJ\ell},\ v_{CJ\ell}) & \text{if left wave = CJ detonation,} \\ (\rho_\ell,\ p_\ell,\ v_\ell) & \text{otherwise,} \end{cases}$$

$$M_r^{\nu+1} = \begin{cases} \sqrt{p_r \rho_r}\, \phi_3(\rho_r \Delta_r, p_r, p_*^{\nu+1}) & \text{if right wave = strong detonation,} \\ \sqrt{\tilde{p}_r \tilde{\rho}_r}\, \phi(p_*^{\nu+1}/\tilde{p}_r) & \text{otherwise,} \end{cases}$$

$$M_\ell^{\nu+1} = \begin{cases} \sqrt{p_\ell \rho_\ell}\, \phi_3(\rho_\ell \Delta_\ell, p_\ell, p_*^{\nu+1}) & \text{if left wave = strong detonation,} \\ \sqrt{\tilde{p}_\ell \tilde{\rho}_\ell}\, \phi(p_*^{\nu+1}/\tilde{p}_\ell) & \text{otherwise.} \end{cases}$$

The complexity of this iteration is more apparent than real. It is stopped when it has converged, as before. New values of Z_{*r}, $Z_{*\ell}$, Δ_r, Δ_ℓ are evaluated, and the iteration is repeated; this process is stopped when Δ_r, Δ_ℓ change by less than some predetermined ε_3 over two successive iterations. It can be readily seen that with the present expression for the energy of formation, at most four iterations on Δ_r, Δ_ℓ are ever needed.

Once S_* has been determined, the solution must be sampled. Let $P = (\theta h, k/2)$ be the sample point, and $\tilde{\rho} = \rho(P)$, $\tilde{p} = p(P)$, etc. Four basic cases are to be considered:

A) P lies to the right of the slip line and the right wave is either a shock or a strong detonation;

B) P lies to the right of the slip line and the right wave is either a rarefaction or a CJ detonation followed by a rarefaction;

C) P lies to the left of the slip line and the left wave is either a shock or a strong detonation, and

D) P lies to the left of the slip line and the left wave is either a rarefaction or a CJ detonation followed by a rarefaction.

Case A. The velocity U_r of the shock or the strong detonation can be found from the relationship

$$M_r = -\rho_r(v_r - U_r);$$

if P lies to the right of $\frac{dx}{dt} = U_r$ we have the sampled values $\tilde{\rho} = \rho_r$, $\tilde{p} = p_r$, $\tilde{v} = v_r$, $\tilde{Z} = Z_r + \delta Z_r$. If P lies to the left of $\frac{dx}{dt} = U_r$, we have $\tilde{\rho} = \rho_{*r}$, $\tilde{p} = p_*$, $\tilde{v} = v_*$, $\tilde{Z} = Z_{*r}$.

Case B. Consider first the case of a rarefaction wave. The rarefaction s bounded on the right by the line $\frac{dx}{dt} = v_r + c_r$, $c_r = \sqrt{\gamma p_r/\rho_r}$, and on the left by $\frac{dx}{dt} = v_* + c_{*r}$, where c_* can be found by using the constancy of the Riemann invariant

$$\Gamma_r = 2c^*(\gamma-1)^{-1} - v_* = 2c_r(\gamma-1)^{-1} - v_r.$$

If P lies to the right of the rarefaction, $\tilde{\rho} = \rho_r$, $\tilde{p} = p_r$, $\tilde{v} = v_r$, $\tilde{Z} = Z_r + \delta Z_r$. If P lies to the left of the rarefaction, $\tilde{\rho} = \rho_{*r}$, $\tilde{p} = p_*$, $\tilde{v} = v_*$, $\tilde{Z} = Z_r + dZ_r$. If P lies inside the rarefaction, we equate the slope of the characteristic $\frac{dx}{dt} = v + c$ to the slope of the line through the origin and P, obtaining

$$\tilde{v} + \tilde{c} = 2\theta h/k;$$

the constancy of Γ_r, the isentropiclaw $p\rho^{-\gamma}$ = constant and the definition

$c = \sqrt{\gamma p/\rho}$ yield $\tilde{\rho}$, $\tilde{v}$, and $\tilde{p}$. $\tilde{Z} = Z_r + \delta Z_r$. If the wave is a CJ detonation, (ρ_r, p_r, v_r) are replaced everywhere by $(\rho_{CJr}, p_{CJ}, v_{CJ})$, and $\tilde{Z}$ inside the fan and to the left of it equals Z_{*r}.

The cases C and D are mirror images of A and B, and will not be described in full.

Numerical results.

We begin by presenting some results for detonation waves with very large K_0 ($K_0 = 1000$). These results verify the accuracy of the programming rather than the general validity of the method, since the solutions of the corresponding problems are an intrinsic part of the Riemann problem solution routine.

To obtain table I, I started with a gas at rest, $\rho = 1$, $v = 1$, $p = 1$, and at $t = 0$ imposed impulsively on the left the boundary condition $v = V = 1$. I used $h = 1/7$, $k/h = 2$, $K_0 = 1000$, $T_0 = 1.1$, $q = 1$ and $\gamma = 1.4$. The result is a perfect strong detonation.

In table II a Chapman Jouguet detonation is exhibited. $h = 1/9$, $k/h = 2$, $K_0 = 1000$, $T_0 = 1.1$, $q = 12$ and $\gamma = 1.4$. $m = 11$. The solution is exhibited at $t = 2$, $n = t/k = 9$, i.e. n is not a multiple of m and the solution is not at its most accurate. This can be seen from the presence of a fake constant state (for $x = 6/9$ and $7/9$), which was discussed in the section about errors, and which is most likely to appear when n is not a multiple of m. The last column presents the right Riemann invariant Γ_r which is of course constant behind the CJ front. The chemical time scale is not resolved on the grid, and one should notice the small number of mesh points required to display sharp variations in all quantities.

Table I

Strong Detonation

$h = 1/7$, $k/h = .2$, $t = nk = .314$, $n = 11$, $K_0 = 1000$, $T_0 = 1.1$, $V = 1$, $q = 1$, $\gamma = 1.4$.

x	v	ρ	p	T	Z
0	1.	1.814	3.228	1.779	.000
1/7	1.	1.816	3.228	1.779	.000
2/7	1.	1.816	3.228	1.779	.000
3/7	1.	1.816	3.228	1.779	.000
4/7	0.	1.000	1.000	1.000	1.000
5/7	0.	1.000	1.000	1.000	1.000
6/7	0.	1.000	1.000	1.000	1.000
1	0.	1.000	1.000	1.000	1.000

Table II

Chapman Jouguet Detonation

$h = 1/9$, $k/h = .2$, $t = nk = .2$, $n = 9$, $K_0 = 1000$, $T_0 = 1.1$, $V = 1$, $q = 12$, $\gamma = 1.4$

x	v	ρ	p	T	Z	Γ_r
0	1.000	1.179	6.965	5.907	0.000	13.379
1/9	1.000	1.179	6.965	5.907	0.	13.379
2/9	1.000	1.179	6.965	5.907	0.	13.379
3/9	1.000	1.179	6.965	5.907	0.	13.379
4/9	1.186	1.257	7.621	6.061	0.	13.379
5/9	1.251	1.287	7.862	6.115	0.	13.379
6/9	1.524	1.410	8.952	6.346	0.	13.379
7/9	1.524	1.410	8.952	6.346	0.	13.379
8/9	1.623	1.457	9.373	6.430	0.	13.379
1	0.	1.000	1.000	1.000	1.000	5.916

We now present some results for a problem whose solution is not programmed into the solution algorithm—a deflagration wave with finite reaction rate. For $t < 0$ a gas at rest lies in $x \geq 0$, with $\rho = 1$, $p = 1$, $(v = 0)$, and $Z = 1$; the left boundary is maintained at zero velocity, $V = 0$. At $t = 0$ the gas in the first cell to the left is raised to a temperature $T = 2$, (i.e. the pressure is increased to $p = 2$). The resulting deflagration wave is observed. It is known that the velocity of the wave is asymptotically proportional to $\sqrt{\lambda K_0}$ (see e.g. [10] p. 99); thus, the wave does not propagate unless $\lambda \neq 0$, as one can readily verify on the computer. This last justifies an earlier assertion to the effect that when $\lambda = 0$ the wave is indistinguishable from a slip line. The results in Table III were obtained with $h = 1/11$, $k/h = .35$, $T_0 = 1.6$, $K_0 = 1$, $q = 10$, $\gamma = 1.4$ and $m = 11$. They are presented at $t = nk = .273$, $(n = q)$. One can clearly see the precursor shock, and the deflagration zone (characterized by $Z < 1$) in which the density and pressure decrease. The small number of mesh points should again be noticed.

Table III

A deflagration with finite conduction and reaction rate.

$h = 1/11$, $k/h = .35$, $t = nk = .273$, $n = 9$, $K_0 = 1$, $T_0 = 1.6$, $V = 0$, $q = 10$, $\gamma = 1.4$.

x	v	ρ	p	T	Z
0	0.	.567	1.667	2.937	.334
1/11	0.139	.650	1.781	2.739	.614
2/11	0.261	.547	1.315	2.402	.614
3/11	.385	1.074	1.726	1.607	1.000
4/11	.575	1.550	1.998	1.288	1.
5/11	.544	1.519	1.800	1.185	1.
6/11	.023	1.016	1.058	1.041	1.
7/11	.002	1.001	1.003	1.002	1.
8/11	.000	1.000	1.000	1.000	1.
9/11	0.	1.	1.	1.	1.
10/11	0.	1.	1.	1.	1.
1	0.	1.	1.	1.	1.

Conclusions.

We have presented a numerical method capable of describing a complex gas flow with chemical reactions. The relative complexity of the method is balanced by economy in the representation of the solution. Generalization of the method to problems in more space dimensions is a straightforward application of the fractional step method presented in [2], and the inclusion of a more realistic chemical process presents no difficulties other than the standard difficulties of finding a plausible kinetic scheme and acceptable numerical values for the corresponding coefficients. The interesting and major difficulties in multidimensional problems arise when one attempts to take into account boundary layers and turbulence effects. In a forthcoming paper we shall show that boundary layer effects at least can be incorporated into our method in a natural and efficient way; once this has been explained, multidimensional results will be presented.

BIBLIOGRAPHY

[1] A. A. Borisov, Acta Astronautica, 1, 909 (1974).

[2] A. J. Chorin, J. Comp. Phys.,

[3] L. M. Cohen, J. M. Short and A. K. Oppenheim, Combustion and Flame, 24, 319 (1975).

[4] R. Courant and K. O. Friedrichs, Supersonic Flow and Shock Waves, Interscience (1948).

[5] J. Glimm, Comm. Pure Appl. Math., 18, 697 (1965).

[6] S. K. Godunov, Mat. Sbornik, 47, 271 (1959).

[7] P. D. Lax, SIAM Review, 11, 7 (1969).

[8] A. Majda and S. Osher, to appear.

[9] R. D. Richtmyer and K. W. Morton, Finite Difference Methods for Initial Value Problems, Interscience (1967).

[10] F. A. Williams, Combustion Theory, Addison Wesley (1965).

List of figure captions

Fig. 1. The Hugoniot curve for exothermic gas flow.

TECHNICAL INFORMATION DIVISION
LAWRENCE BERKELEY LABORATORY
UNIVERSITY OF CALIFORNIA
BERKELEY, CALIFORNIA 94720